Regular Article

Nature of Lithium Interactions with DNA Nucleobases: Theoretical Study

M. Farrokhnia[a,b] and A.H. Pakiari[a,*]

[a]Chemistry Department, College of Science, Shiraz University
[b]The Persian Gulf Marine Biotechnology Research Center, Bushehr University of Medical Sciences, Bushehr, Iran
(Received 2 March 2014, Accepted 4 August 2014)

In the present study, the interactions of three different lithium species Li^+, Li_3^+ and CH_3Li with several different sites of the most stable tautomers of DNA nucleo-bases are presented. This investigation is based on the results of thermochemical properties, Quantum Theory of Atoms in Molecules (QTAIM) and Natural Bond Orbital (NBO) analysis, obtained at B3LYP/6-311++G(d,p) level of theory. The calculated results showed that guanine and cytosine have more tendencies for interaction with lithium in all above three lithium species. Also, it was shown that for each tautomer of the same nucleobase, coordination mode of lithium highly affects the value of Metal Ion Affinity (MIA). Bidentate base has more lithium affinity and the carbonyl oxygen is generally preferred over amino nitrogen. Furthermore, the analysis revealed the electrostatic nature of interactions. *Li^+-DNA-Base* has the most MIA value and *CH_3Li-DNA-Base* has the least one.

INTRODUCTION

The information stored in deoxyribonucleic acid (DNA) indicates that each step required for the organism to construct a replica of itself. DNA contains three important sites including phosphate groups and the sugar part as well as the DNA-*bases*. This is well-known that the coordinated metal ions play a significant role in the biological action of nucleic acids, and directly impact on oxidation-reduction reactions or induce conformational changes indirectly [1]. For instance, alkali metal cations interact with DNA-*bases* and destroy the hydrogen bonded network between the base pairs. Consequently, the structure of DNA will be changed [2-4]. Although metal cations are vital for essential processes and their presence may stabilize the special form of DNA, the improper metal cations or wrong concentration of vital ions may cause undesired effects [5]. As a result of DNA significance in biological environments, knowledge of the thermodynamic, structural, and electronic features which manage the interaction between alkali metal cations and nucleic acid bases, can give useful indication of their interactions with more complex nucleic acid polymers.

The H$^+$ and Li^+ interactions with DNA-*bases* have been investigated by a diversity of experimental and theoretical methods in recent years [6-16]. Experimental gas phase studies on interaction of alkali metal cations including Li^+ with DNA-*bases* have been performed by using different mass spectroscopy methods [9,17-24]. Rodgers and Armentrant have studied the lithium affinities for uracil, thymine and adenine by threshold collision-induced dissociation in Xenon using guided ion beam mass spectrometry and the MP2 computational method [12]. NMR studies of Li^+ interaction with nucleosides have been also reported in literatures [25,26]. Cerda and Wesdemiotis have reported the interaction of Li^+, Na^+ and K^+ with DNA-*bases* by modified version of kinetic methods; however, they did not show the information on the coordination site of metal [16].

Del Bene [27] has published the results of a study for the Li^+ complex of the DNA-*bases* by *ab initio* calculations

---

*Corresponding author. E-mail: pakiariah@gmail.com

with the STO-3G basis sets to determine the optimized structures and stabilization energies. However, their results are not reliable because calculations have been done at the low level of theory and basis set. Zhu and colleagues have theoretically probed the interaction of nucleobase with alkali and alkali earth metal cations [28]. Sun and Bu have shown, at B3LYP level and 6-31+G* basis set, that the coupling of Li^+ to guanine-cytosine base pair can strengthen the interaction between guanine and cytosine [29]. Zhao *et al*. [30] and Reynisson [31] have separately investigated the interaction of guanine-cytosine base pair with metal ions by means of density functional theory (DFT) calculations. Hashemianzadeh *et al*. [32] have also reported some results of interaction between isolated DNA-bases and alkali and alkali earth metal cations by *ab initio* calculation and compared them with experimental results, however, they didn't study the most stable tautomers of DNA-*bases*.

The interaction of small alkali metal clusters with DNA is also interesting because their qualitative properties can be understood from simple models [33-35]. This aspect of *Li* cluster can be considered to study the interaction of small cluster with DNA-*base*. Moreover, CH_3Li is another species which has charged lithium ion (computed between +0.794 and +0.857 from natural population analysis at the DFT level) and binds *via* a lithium bond to the DNA metal coordination sites. Methyllithium has been proposed as a candidate for chemical test of DNA sequencing [36].

In the present study, we would like to theoretically investigate the interaction of DNA-*bases* with Li^+, Li_3^+ and CH_3Li, called *Li* derivatives in this paper. These species have been selected for studying the possibility of DNA-*base* reaction with *Li* derivatives which might help to better understanding of some aspects of DNA identification. We have performed a systematic DFT study in gas phase to compare the energetic and structures of different complexes with above mentioned species. The gas phase has been selected for avoiding the complicated solvent effects which can influence on complexation mechanism, binding energy and reactivity of metal cations. What distinguishes this research from others is characterization of *Li-base* bonds in terms of Quantum Theory of Atoms in Molecules (QTAIM) [37,38] parameters. Furthermore, Natural Bond Orbital (NBO) [39,40] theory has been also used for analyzing the interaction details.

COMPUTATIONAL DETAILS

The geometry of all complexes has been fully optimized by Gaussian03 [41] and visualized using Gaussview 3.0 packages [42]. The calculations have been carried out at the DFT level by using B3LYP functional [43,44] with 6-311++G(d,p) basis set without any symmetry restriction. Vibrational frequencies have been also calculated to confirm that all the stationary points correspond to the true minima on the potential energy surface.

Natural population analysis [45] has been employed to determine total atomic charge on interaction sites in both DNA-*base*s and *Li* compounds, and the charge transfer in these complexes. QTAIM was also applied to reveal bond critical point (BCP) properties and show the nature of *Li*-DNA-*base* interactions by using AIM2000 package [46].

The interaction energy of complexes has been computed by using Eq. (1),

$$\Delta E_{int} = E^{A,metal} - (E^{metal} + E^A) \qquad (1)$$

The letter E stands for total electronic energy of a complex or subsystem. ΔE_{int} means the interaction energy of a complex and A stands for acceptor species. Zero-point corrections have been included in interaction energies. However, the basis set superposition errors (BSSE) are not considered because of their negligible values in alkali metal complexes of DNA-*bases* [12], for example K^+ complexes have the BSSE about 2.0 kcal mol^{-1}.

Metal ion affinity (MIA) is defined as the negative of the enthalpy variation ΔH^{298} for the following processes,

$$B + Metal^{n+} \rightarrow B - Metal^{n+} \; complex \qquad (2)$$
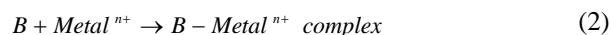
in which B represents a particular DNA-base. $Metal^{n+}$ can be either Li^+, Li_3^+ or CH_3Li. The MIA can correspond to dissociation energy of $B-metal^{n+}$ bond (for example, Li^+-*Base* in the present investigation). Thermodynamic values are considered at 298.15 K in order to obtain entropy contribution ($T\Delta S^{298}$) and free energy variation (ΔG^{298}) for these processes. The evaluation of these thermodynamic values is explained as follow. The best way for considering MIA is to report the thermodynamic properties such as enthalpy variation of the metalation process or interaction

energy of metal and acceptors. The gas-phase interaction enthalpy ΔH^{298} for reaction (2) is defined

$$\Delta H^{298} = \Delta E^{298} + \Delta PV = E^{298}_{B-Metal^{n+}} - E^{298}_{Metal^{n+}} - E^{298}_{B} - RT \quad (3)$$

where $E^{298}_{B-Metal^{n+}}$ is the energy of the complex, $E^{298}_{Metal^{n+}}$ is the energy of respective metal cation and E^{298}_{B} is the energy of the acceptor. Gibbs energy ΔG^{298} of the metal cation coordination reaction may be calculated from,

$$\Delta G^{298} = \Delta H^{298} - T\Delta S^{298} \quad (4)$$

The entropy contribution is given by,

$$-T\Delta S^{298} = -T\left[S(B - Metal^{n+}) - S(Metal^{n+}) - S(B)\right] \quad (5)$$

The Gaussian03 provides the sum of electronic, ε_0, and thermal enthalpies. Then, it is possible to simplify Eq. (5) and take the difference of the sums of these values for the reactants and the products.

$$\Delta H^{298} = \sum\left(\varepsilon_o + H_{corr}\right)_{product} - \sum\left(\varepsilon_o + H_{corr}\right)_{reactant} \quad (6)$$

The same short cut can be used to calculate Gibbs free energies of reaction:

$$\Delta G^{298} = \sum\left(\varepsilon_o + G_{corr}\right)_{product} - \sum\left(\varepsilon_o + G_{corr}\right)_{reactant} \quad (7)$$

where ε_0 is the total electronic energy, H_{corr} is correction to the enthalpy due to internal energy, G_{corr} is correction to the Gibbs free energy due to internal energy in both Eqs. (6) and (7).

RESULTS AND DISCUSSION

Lithium Affinity

As the first step of the present work, thermochemical quantities of metalation reaction are calculated. We considered the nucleic acid *bases* in their most usual configurations in DNA-*base* pairs as shown in Fig. 1, according to the configurations used in experimental work of Cerda and Wesdemioties [11,16] and *ab initio* study of
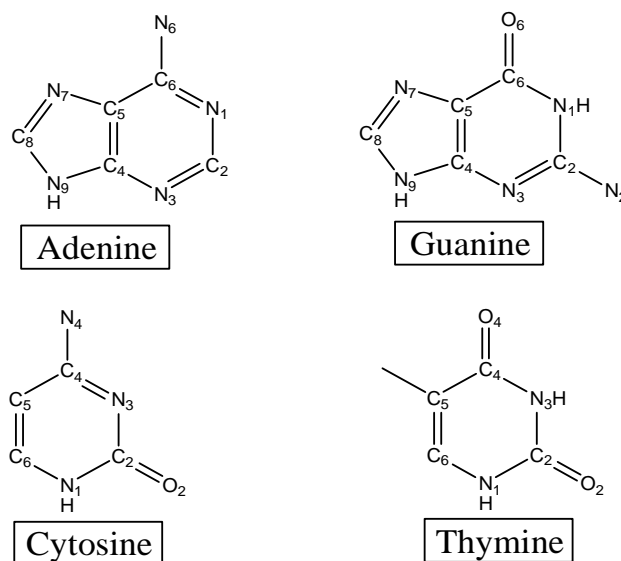


Fig. 1. DNA nucleobases and labeling.

Russo *et al.* [14].

The nomenclatures of complexes are shown in Figs. 2 to 4. In each complex, the first part of the name stands for tautomer name and depends on the position of H atom attached to nitrogen involving in tautomerization reaction. For examples ade-N_1, ade-N_3, ade-N_7 and ade-N_9 are four different tautomers of adenine which are studied in the present study. The second part of the name includes the lithium derivative types attached to the base tautomer and the involved coordination sites of each tautomer. In the case of adenine, ade-N_9-Li^+-N_6-N_7 refers to bidentate interaction of Li^+ with ade-N_9 with coordination sites N_6 and N_7. Similar nomenclature is applied for the rest of bases and their complexes. But, for the sake of simplicity, the complexes are reported in tables by smaller notation "combing number and letter a, b and c" as mentioned in Figs. 2 to 4. "a" stands for Li^+-*complexes,* "b" for Li_3^+-*complexes and* "c" for *CH_3Li-complexes.* The number refers to each complex in the table.

To demonstrate interaction site for metalation of these DNA-*bases*, we computed lithium affinities MIA (-ΔH^{298}) at several sites of tautomers. The results of calculated lithium affinities MIA, free energy variations ΔG^{298}, entropic contributions ΔS^{298} and interaction energies ΔE^{298}, at 298.15 K, are presented in Table 1. The optimized
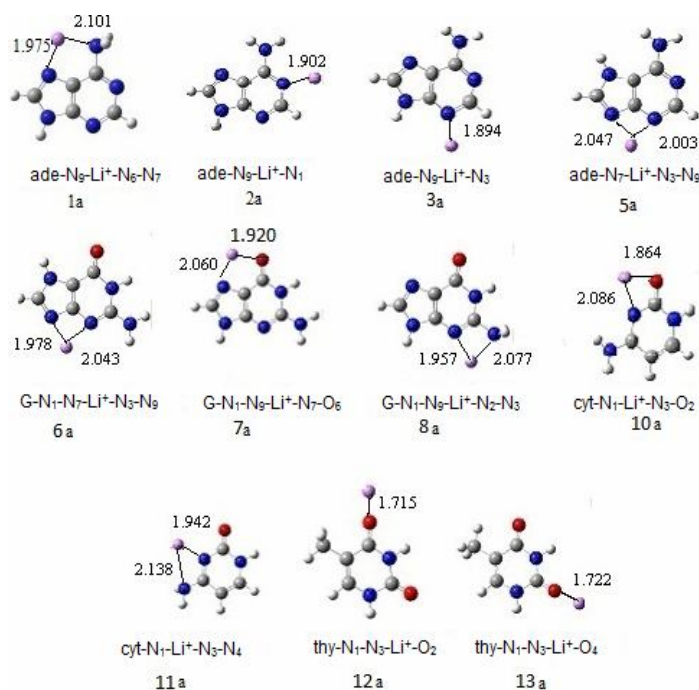
Fig. 2. Optimized geometry of Li^+ complexes at B3lYP/6-311++G** level. Distances are in angstrom.
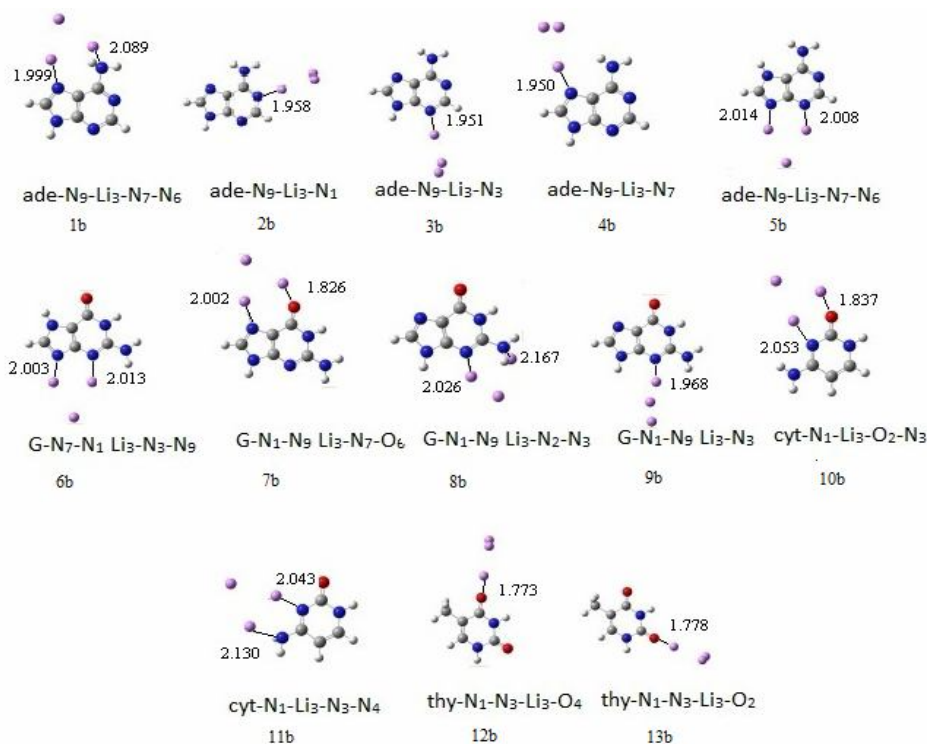
Fig. 3. Optimized geometry of Li_3^+ complexes at B3LYP/6-311++G** level (in above figure 1b-13b, Li_3 is actually Li_3^+). Distances are in angstrom.
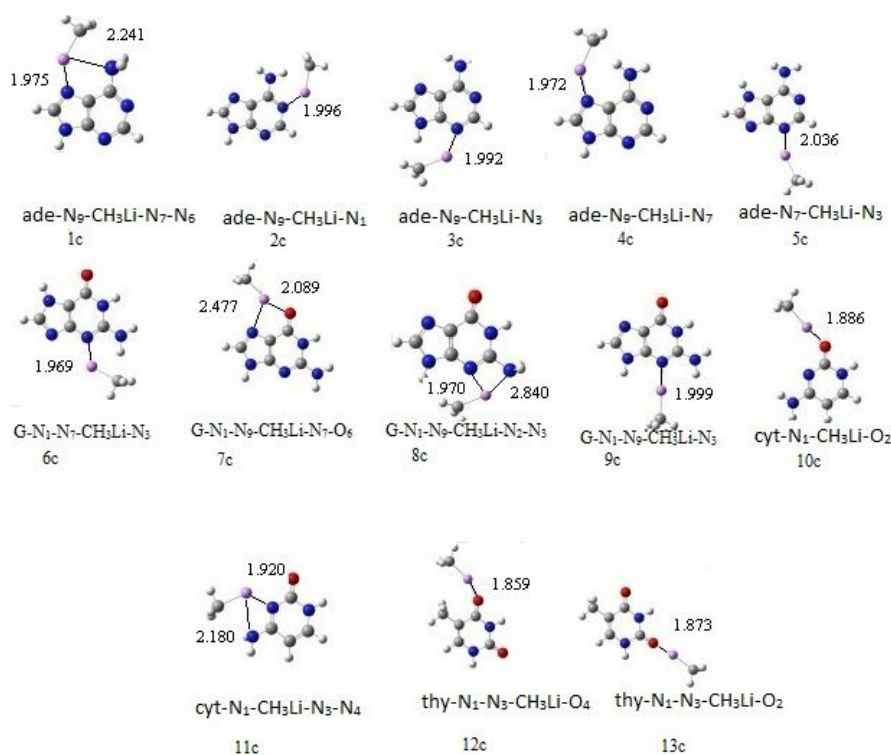
Fig. 4. Optimized geometry of *CH₃Li* complexes at B3LYP/6-311++G** level. Distances are in angstrom.

Table 1. Thermochemistry Properties of Complexes[a]

Complex	Complex with Li^+				Complex	Complex with Li_3^+				Complex	Complex with *CH3Li*			
	$-\Delta H^{298}$†	$-\Delta G^{298}$	$-T\Delta S^{298}$	$-\Delta E_{int}$		$-\Delta H^{298}$†	$-\Delta G^{298}$	$-T\Delta S^{298}$	$-\Delta E_{int}$		$-\Delta H^{298}$†	$-\Delta G^{298}$	$-T\Delta S^{298}$	$-\Delta E_{int}$
1a	50.624	41.816	8.804	49.512	1b	33.512	20.250	13.262	32.831	1c	24.504	13.446	11.064	26.314
2a	45.201	36.202	8.998	44.082	2b	28.896	20.006	8.890	29.156	2c	24.359	14.340	10.019	26.311
3a	45.216	36.953	8.263	44.407	3b	29.143	19.611	9.532	29.240	3c	26.901	17.533	9.367	29.049
4a	-	-	-	-	4b	26.455	16.811	9.644	26.513	4c	24.504	13.777	10.727	26.339
5a	65.567	57.864	7.703	64.958	5b	51.056	39.504	11.553	50.943	5c	21.851	12.844	9.007	23.957
6a	62.511	55.312	7.199	62.093	6b	45.489	34.403	11.086	45.508	6c	28.874	19.779	9.094	31.181
7a	73.412	65.799	7.613	72.823	7b	58.306	47.287	11.018	58.329	7c	22.375	16.158	6.216	25.054
8a	40.624	32.917	7.706	39.859	8b	20.822	9.523	11.299	20.682	8c	18.006	9.798	8.208	19.691
9a	-	-	-	-	9b	19.685	11.254	8.432	20.168	9c	17.364	6.688	10.675	18.993
10a	68.532	60.695	7.836	67.920	10b	52.678	41.813	10.865	52.712	10c	24.093	17.372	6.721	26.958
11a	47.722	39.152	8.570	46.704	11b	51.668	40.609	11.059	51.695	11c	30.103	21.152	8.951	32.499
12a	52.582	45.991	6.591	52.391	12b	34.302	27.076	7.226	35.079	12c	21.387	13.637	7.749	23.839
13a	49.396	42.104	7.292	48.853	13b	32.729	25.378	7.351	33.529	13c	20.205	12.302	7.903	22.687

[a]All calculated thermochemistry properties are reported in kcal mol⁻¹. †As it is mentioned in the text, we have assumed the MIA as the negative of the enthalpy variation ΔH^{298}. So that -ΔH^{298} refers to MIA values.

geometries of all complexes are illustrated in Figs. 2 to 4.

The ground state of Li_3^+ was optimized without imposing any symmetry, and obtained almost D_{3h} symmetry. Its total energy is -22.3721 a.u. with bond length 2.952 Å. Charge on each atom is 0.33. CH_3Li is another species which has total energy -47.4200 a.u. and C-Li bond length 1.972 Å and charge on Li is 0.49 a.u. So that, the interaction of Li^+, Li_3^+ and CH_3Li with several DNA-*base* tautomers will be probed in the below.

For Li^+ complexes, both mono and bidentate interactions are detected. The metal cation coordination sites are mainly the N_7, N_9, and O_6 atoms of guanine and adenine, the O_4 atom of thymine, and the N_3 and O_2 for cytosine when the hetero atoms are not involved in hydrogen bonding [14]. The optimized geometries of all complexes and thermodynamic values are presented in Fig. 2 and Table 1. In adenine series, two bidentate complexes, ade-N_9-Li^+-N_6-N_7, (1a), and ade-N_7-Li^+-N_3-N_9, (5a), have more MIAs and interaction energies. The MIAs are -50.62 and 65.57 kcal mol^{-1}, respectively. However, the N_3 and N_9 atoms are more favorable interaction sites for lithium cation. Although ade-N_7 tautomer is not the most stable configuration of adenine, it has relative energy about -8.391 kcal mol^{-1} with respect to ade-N_9, and its bidentate complex has the highest lithium affinity.

In guanine series, complexation with the G-N_1-N_9 tautomer has more MIA and also corresponds to the bicoordination of the lithium cation with O_6 and N_7 in G-N_1-N_9-Li^+-N_7-O_6, (7a), -73.41 Kcal mol^{-1}. In guanine tautomers, lithium tends to have bidentate interaction with all different sites. Unlike adenine case, the least MIA value corresponds to the least stable tautomer of guanine in (8a).

Cytosine has the same condition as the guanine. It prefers to interact with both possible coordination sites simultaneously. In accordance with the results in Table 1, cyt-N_1-Li^+-N_3-O_2, (10a), has more interaction energy and MIA. Finally, two thymine complexes are mono-coordinated but O_4 atom is preferred in (12a).

Comparing lithium cation Li^+ affinities in Table 1 gives the order guanine > cytosine > adenine > thymine which seems sensible because there are more possibilities in guanine and cytosine molecules to have bidentate complex. These interactions form five-membered ring in guanine and four-membered ring in cytosine. In principle, the five-membered ring formation is favored with respect to that of four-membered one because of the minor annular strain. Furthermore, interaction of Li^+ is more effective with nitrogen or oxygen atoms having a noticeable negative charge.

Li_3^+-*Base* complexes have the same interaction sites and trend as Li^+-*Base* complexes, shown in Fig. 3. The computed results in Fig. 3 and Table 1 show that the ade-N_7-Li_3^+-N_3-N_9, (5b), and G-N_1-N_9-Li_3^+-N_7-O_6, (7b) complexes have the most interaction energies and also have MIA values in adenine and guanine series, respectively. Cyt-N_1-Li_3^+-O_2-N_3, (10b), and thy-N_1-N_3-Li_3^+-O_2, (12b), have also more interaction energy and have MIA values with respect to their alternative tautomers. The Li_3^+ geometry varies during interaction with DNA-*base* but the changes depend on the tautomer and its active sites. The D_{3h} symmetry of Li_3^+ is destroyed in these interactions. The symmetry of monodentate interactions such as in complexes 2b, 3b, 4b, 12b or 13b are changed to almost C_{2v}. However, Li_3^+ loses its D_{3h} symmetry in all bidentate interactions completely.

In CH_3Li-*Base* complexes, methyllithium almost has monodentate interaction with active sites. From the results in Table 1, the most lithium affinity in adenine series belongs to ade-N_9-CH_3Li-N_3 (3c) complex, -26.90 kcal mol^{-1}. Guanine complexes have two types of interactions with methyllithium, monodentate such as G-N_1-N_7-CH_3Li-N_3 (6c), which has highest MIA value -28.87 kcal mol^{-1}, and bidentate such as G-N_1-N_9-CH_3Li-N_3 (7c), which has the lowest MIA value in Guanine complex, -17.36 kcal mol^{-1}. The N_3 and N_4 sites in cytosine, cyt-N_1-CH_3Li-N_3-N_4,(11c), which has the most MIA value -30.10 kcal mol^{-1}, sound to be better electron donor to CH_3Li and their MIA are more than O_2 site in cyt-N_1-CH_3Li-O_2, (10c), with MIA -24.09 kcal mol^{-1}. In thymine complexes, it is interesting that O_4 atom interacts with methyllithium with a little more MIA than O_2, thy-N_1-N_3 CH_3Li-O_4 (12c), -21.39 kcal mol^{-1}, while in thy-N_1-N_3 CH_3Li-O_2, (13c), -20.21 kcal mol^{-1}. The MIA value order in CH_3Li complexes is cytosine > guanine > adenine > thymine.

The results of Table 1 indicate that, for all DNA-*bases*, the MIA values depend on the considered tautomers and the

coordination mode of lithium. The trend for lithium affinity in three different lithium species is generally $Li^+ > Li_3^+ > CH_3Li$. The trend in MIA among the identical DNA-*base* (with few exception for CH_3Li-*base* complexes in 1c, 3c, 6c and 7c) is:

Bidentate with N and O > Bidentate with both N inside of the rings > Bidentate with two N inside and outside > single with O > single with N.

Thermochemistry Analysis

There are series of difficulties for experimental measurement of MIA [47] preventing the evaluation of the entropic effect, but theoretically all thermochemical properties can be computed at any desired temperature. Entropic contributions are necessary for determining the free energy. Table 1 contains also Gibbs free energies ΔG^{298} and entropies ΔS^{298}. Gibbs free energy itself can give acidity, $(PK_a = -\Delta G^{298}[H^+]/2.303RT)$, and the more negative ΔG^{298} shows the higher Lewis acidity. Since the value of $-T\Delta S^{298}$ is small, the relative differences between ΔG^{298} values are similar to ΔH^{298}. Therefore, acidity can be attributed to MIA. On the whole, the lithium acidity or ΔG^{298} values follow the same trend as MIAs, the more acidic of lithium species, the higher affinity of DNA-*base* interaction sites, $Li^+ > Li_3^+ > CH_3Li$.

It is possible to evaluate ΔS^{298} from data in Table 1. ΔS^{298} Values for different Li^+ complexes vary from 22.14 to 30.20 cal (mol^{-1} K^{-1}). The corresponding values for Li_3^+ complexes are between 24.26 and 44.50 cal (mol^{-1} K^{-1}) and for CH_3Li series, is between 20.87 and 37.11 cal mol^{-1} K^{-1}. In other words, the difference between the maximum and minimum values of ΔS^{298} are 8.1, 20.24 and 16.22 cal (mol^{-1} K^{-1}) for Li^+, Li_3^+ and CH_3Li, respectively.

Quantum Theory of Atoms in Molecules Analysis

In this part of our research, bond critical point (BCP) was analyzed in terms of the following characteristics [38]: The electronic density $\rho(r)$ at the critical point (CP), its Laplacian, which is related to the bond interaction energy by a local expression of the virial theorem is $\nabla^2_{\rho_{BCP}} = 2G + V$. The total electronic energy density at the CP is $H(r) = G + V$. For Laplacian $\nabla^2_{\rho_{BCP}}$ and total electronic energy $H(r)$ expressions, (V) is the potential electronic energy density

(V) and must be negative and (G) is the electronic kinetic energy density which is always positive [48,49]. Delocalization indices were also calculated for Li-Li bonds in Li_3^+ complexes. When Laplacian $\nabla^2_{\rho_{BCP}}$ and H are both positive, the bond is electrostatic (closed shell), or if both are negative, the bond should be covalent. But, if $\nabla^2_{\rho_{BCP}}$ is positive and H is negative, the bond is partial electrostatic and partial covalent.

According to QTAIM results in Table 2 for Li^+ complexes, in all bidentate DNA-*base* tautomers with two BCPs have been detected. The minimum density ρ_{BC} of Li-N for Li-N$_4$ is between 2.185×10^{-2} in (11a) and the maximum is 4.785×10^{-2} in (3a). Li-O interaction possesses more ρ_{BC} than Li-N interaction. Its minimum value density is 3.178E-2 in G-N$_1$-N$_9$-Li$^+$-N$_7$-O$_6$ (7a) and Li-O$_4$ interaction has the maximum ρ_{BC} 4.69E-2 in thy-N$_1$-N$_3$-Li$^+$-O$_4$ (12a). Consequently, all positive $\nabla^2 \rho_{BC}$ are a criterion of electrostatic interactions. Li-O interaction plays an important role in complexation.

Table 3 shows the QTAIM parameters of Li_3^+ series. The values of ρ_{BC} in Li_3^+ series are less than their corresponding values in Li^+. These evidences also reveal that Li^+ interaction with similar active site has stronger interaction than Li_3^+ and CH_3Li complexes. In a similar way to Li^+-DNA-*base* interaction, in Li_3^+ series, Li interaction is electrostatic bond. As it can be shown from results in Table 4, the interaction of DNA-*base* with CH_3Li creates one BCP between Li and *base* in all complexes. BCPs of Li-N$_7$ (1c) in adenine and Li-N$_3$ (6c) in guanine own the most ρ_{BC}. The minimum ρ_{BC} for Li-N and Li-O interactions belong to ade-N$_7$-CH$_3$Li-N$_5$ (5c) and G-N$_1$-N$_9$-CH$_3$Li-N$_7$-O$_6$ (7c), respectively. Interesting point is that the trend in $\nabla^2 \rho_{BC}$ of three types complexes reveal the same trend as MIA (but not linear), as the following;

$$Li^+ \text{DNA-}base > Li_3^+ \text{DNA-}base > CH_3Li \text{DNA-}base$$

For more detailed study of Li-interactions, we have also considered the change of bond properties in Li_3^+ and CH_3Li. These properties are the bond distances (in angstrom) and delocalization indices (DI in a.u.) which indicates the electron density of corresponding chemical

Table 2. BCP Properties of Li^+-DNA-*Base* Interaction[a]

Molecule	Bond	ρ_{BC} [-2]	$H_{BCP}(r)$ [-2]	$\nabla^2\rho_{BC}$ [-1]
1a	Li-N$_7$	3.043	0.752	1.945
	Li-N$_6$	2.532	0.521	1.423
2a	Li-N$_1$	4.065	0.772	2.542
3a	Li-N$_3$	4.785	0.799	2.611
5a	Li-N$_3$	2.435	0.695	1.773
	Li-N$_9$	2.362	0.658	1.529
6a	Li-N$_3$	2.435	0.644	1.552
	Li-N$_9$	2.871	0.754	1.884
7a	Li-N$_7$	2.406	0.614	1.481
	Li-O$_6$	3.178	0.847	2.124
8a	Li-N$_3$	3.193	0.762	2.071
	Li-N$_2$	2.520	0.588	1.528
10a	Li-N$_3$	2.250	0.567	1.415
	Li-O$_2$	3.713	1.058	1.756
11a	Li-N$_3$	3.410	0.803	2.223
	Li-N$_4$	2.185	0.493	1.283
12a	Li-O$_4$	4.690	1.785	4.197
13a	Li-O$_2$	4.579	1.778	4.106

ported properties are in atomic unit (a.u.). [-x] means that the reported values should
be multiplied by 10^{-x}.

Table 3. BCP Properties of Li_3^+-DNA-*Base* Interaction

Molecule	Bond	ρ_{BC} [-2]	$H_{BCP}(r)$ [-2]	$\nabla^2\rho_{BC}$ [-1]
1b	Li-N$_7$	3.011	0.722	1.866
	Li-N$_6$	2.465	0.567	1.438
2b	Li-N$_1$	3.510	0.709	2.127
3b	Li-N$_3$	3.520	0.736	2.164
4b	Li-N$_7$	3.509	0.753	2.172
5b	Li-N$_3$	2.991	0.705	1.834
	Li-N$_9$	2.880	0.716	1.788
6b	Li-N$_3$	2.928	0.682	1.783
	Li-N$_9$	3.003	0.724	1.860
7b	Li-N$_7$	2.986	0.723	1.849
	Li-O$_6$	3.566	1.346	2.902
8b	Li-N$_3$	2.824	0.763	2.071
	Li-N$_2$	1.999	0.487	1.149
9b	Li-N$_3$	3.330	0.709	2.038
10b	Li-N$_3$	2.565	0.621	1.545
	Li-O$_2$	2.682	0.717	1.756
11b	Li-N$_3$	3.306	0.801	2.170
	Li-N$_4$	2.170	0.487	1.263
12b	Li-O$_4$	3.951	1.544	3.395
13b	Li-O$_2$	3.873	1.529	3.327

[a]All reported properties are in atomic unit (a.u.). [-x] means that the
reported values should be multiplied by 10^{-x}.

Table 4. BCP Properties of CH_3Li-DNA-*Base* Interaction[a]

Molecule	Bond	ρ_{BC} [-2]	$H_{BCP}(r)$ [-2]	$\nabla^2 \rho_{BC}$ [-1]
1c	Li-N$_7$	3.162	0.735	1.975
2c	Li-N$_1$	3.115	0.691	+1.902
3c	Li-N$_3$	3.045	0.698	+1.878
4c	Li-N$_7$	3.162	0.737	+1.973
5c	Li-N$_3$	2.738	0.654	+1.659
6c	Li-N$_3$	3.247	0.682	+1.783
7c	Li-O$_6$	2.670	0.856	+1.885
8c	Li-N$_3$	3.073	0.675	+1.790
9c	Li-N$_3$	3.059	0.662	+1.839
10c	Li-O$_2$	3.251	1.250	+2.255
11c	Li-N$_3$	3.278	0.768	+2.077
12c	Li-O$_4$	4.071	0.071	+1.814
13c	Li-O$_2$	3.048	1.214	+2.490

[a]All reported properties are in atomic unit (a.u.). [-x] means that the reported values should be multiplied by 10^{-x}.

Table 5. CH_3-Li Bond Properties, Bond Distances of Li_3^+ in Different Complexes. Bond Delocalization Index δ (in a.u.) and Bond Distances (in Angstrom)

Mol.	$r_{Li1-Li2}$	$r_{Li2-Li3}$	$r_{Li3-Li1}$	$\delta_{Li1-Li2}$ [-2]	$\delta_{Li2-Li3}$ [-2]	$\delta_{Li3-Li1}$ [-2]	Mol.	r_{C-Li}	ρ_{Bc}^{C-Li} *
Li_3^+	2.952	2.951	2.951	4.576	3.981	4.838	CH_3Li	1.971	4.321
1b	3.015	2.920	2.912	2.428	4.094	4.436	1c	2.013	4.071
2b	3.018	2.851	3.018	2.928	6.278	2.933	2c	2.025	3.930
3b	3.019	2.853	3.019	2.961	6.371	2.961	3c	2.036	3.756
4b	3.017	2.863	3.012	2.857	6.003	2.926	4c	2.016	3.994
5b	3.014	2.757	2.927	2.485	4.478	4.503	5c	2.010	4.069
6b	2.934	2.902	2.690	2.657	4.365	4.878	6c	2.041	3.247
7b	2.919	2.926	2.905	2.350	4.810	4.690	7c	1.997	4.124
8b	2.947	2.798	2.914	2.747	3.900	4.349	8c	1.998	4.195
9b	3.019	2.864	3.026	2.880	5.980	2.980	9c	1.995	4.210
10b	2.947	2.914	2.798	2.654	4.850	5.094	10c	2.020	3.667
11b	2.940	2.912	2.780	2.640	4.830	5.194	11c	2.047	2.326
12b	3.204	2.843	3.204	3.073	6.937	3.075	12c	2.009	4.071
13b	3.201	2.863	3.201	3.102	6.783	3.107	13c	2.006	4.100

[-2] means that the reported values should be multiplied by 10^{-2}. *means ρ_{Bc}^{C-Li} should multiply by 10^{-2}.

bond. These results are collected in Table 5. When DI increases, bond distance will decrease and *vice versa*. It is similar with bond order. When bond order increases, bond distance will decrease. Therefore, high Di means the interaction is strong, and high MIA is expected. There are two types of interactions: 1- if bond length is getting to decrease, it means the bond accepts electron, it can call it acceptor bond (back bonding), such as in Li_3^+ in 1b in Table 5, $r_{Li2-Li3} = 2.920$ Å and $r_{Li3-Li1} = 2.912$ Å, which are correspond to DI 4.094 and 4.436 a.u., respectively (comparing with DI 3.981 and 4.838 a.u., and also $r_{Li2-Li3} = 2.951$ Å and $r_{Li3-Li1} = 2.951$ Å of Li_3^+). 2- If bond length is getting to increase, it means the bond is electron donor bond (hyperconjugation), it can call it donor bond, such as in *CH₃Li-compex* in 1c in Table 5, $r_{C-Li} = 2.013$ Å, which corresponds to DI = 4.071 a.u. (comparing with DI = 4.321 a.u. and $r_{C-Li} = 1.971$ Å for *CH₃Li*).

The additional point is that the largest change in bond length or DI, roughly means the large MIA, or *vice versa*. For example, 11c has the largest change in bond length 2.047 Å or in DI = 2.326 a.u. for *CH₃Li-complex*, and therefore the largest change MIA = 30.10 Kcal mol^{-1} is expected in Table 1, (for smallest change in bond length 1.995 or DI 4.210 a.u. in 9c, the smallest MIA 17.36 Kcal mol^{-1} is expected). It is seen the same point for Li_3^+-complexes; for instance in 10b and 9b.

Natural Population Analysis

Atomic charges have been calculated through NBO, based on natural population analysis (NPA). The electron population of each atom was calculated as the sum of the occupation numbers of all the natural atomic orbitals (NAOs) corresponding to that atom. The interacting Li atom in all complexes has the positive charge and the connected atom X (N or O) has the negative charge, showing the electrostatic nature of Li-X bond. The changes of atomic charge on Li species after complexation are shown in Tables 6 to 8. For Li^+-*DNA-base* complexes, the atomic charge of Li^+ becomes less positive and the smallest $\Delta q_{Li^+} = q_{Li^+(complex)} - q_{Li^+(isolated)}$ belongs to thymine complexes while highest value is for G-N₁-N₇-Li⁺-N₃-N₉ (6a), as shown in Table 6.

In Li_3^+ complexes, the overall charge of Li_3^+ cluster reduces and the maximum reduction occurs for G-N₁-N₇-Li_3^+-N₃-N₉ (6b) complex with $\Delta q_{Li_3^+} = q_{Li_3^+(complex)} - q_{Li_3^+(isolated)}$ equal to -0.068 (a.u.). Similar to Li^+ complexes, thymine complex has also the minimum reduction, as shown in Table 7. In all complexes, the atomic charge of Li participating in interaction becomes more positive than others. These changes are in accord with the overall positive charge reduction observed over complexation.

CH₃Li complexes have different behavior and their *Li* positive charges are enhanced in some cases. The maximum reduction of Li atomic charge is $\Delta q_{Li} = -0.084$ which is owned by G-N₁-N₉-CH₃Li-N₃ (9c). From the computed atomic charge in Table 8, there is a change of charge distribution in *CH₃Li* after complexation. Hence, negative charge of C in *CH₃Li* is reduced after complexation, and the maximum decrease is $\Delta q_C = 0.052$ (a.u), in both 5c and 9c. During complexation, the *CH₃Li* geometry changes from its tetrahedral, which are imposed by new charge distribution on *CH₃Li*.

Natural Bond Orbital Analysis

A useful aspect of the NBO method is that it provides information about the interactions in both filled and virtual orbitals that facilitates the analysis of intra- and intermolecular interactions. A second-order perturbation theory analysis of the Fock-matrix helps to study the donor-acceptor interaction in the NBO basis. The interaction results in a loss of occupancy from the localized NBOs of the ideal Lewis structure into the empty non-Lewis orbitals. The stabilization energy ΔE_{CT} for each donor NBO *(i)* and acceptor NBO (*j*) can be evaluated by Eq. (7). The quantities of transferred charge from a donor to a given acceptor orbital can be estimated by Eq. (8).

$$E^{(2)} = \Delta E_{ij} = \Delta E_{CT} = -2\frac{\langle i|F|j\rangle^2}{\varepsilon_j - \varepsilon_i} \tag{7}$$

$$q_{CT} \approx 2\left(\frac{\langle i|F|j\rangle}{\varepsilon_j - \varepsilon_i}\right)^2 \tag{8}$$

The quantities of transferred charge from DNA-*base* active sites to Li acceptor orbital (Δq_{CT}) and their

Table 6. Δq_{CT} (a.u.), ΔE_{CT} (kcal mol^{-1}) of Li^+, q_{Li} (NPA Atomic Charge) and Δq_{Li^+} of Li^+ Complexes in Accordance with Fig. 2

Molecule	Donor to acceptor	Δq_{CT}	ΔE_{CT}	q_{Li}	Δq_{Li^+}
1a	$n_{N7} \rightarrow n_{Li}^*$	0.028	9.61	+0.946	-0.054
	$n_{N6} \rightarrow n_{Li}^*$	0.027	9.11		
2a	$n_{N1} \rightarrow n_{Li}^*$	0.022	8.53	+0.967	-0.033
3a	$n_{N3} \rightarrow n_{Li}^*$	0.021	8.34	+0.968	-0.032
5a	$n_{N3} \rightarrow n_{Li}^*$	0.025	8.17	+0.945	-0.055
	$n_{N9} \rightarrow n_{Li}^*$	0.021	7.26		
6a	$n_{N3} \rightarrow n_{Li}^*$	0.026	8.30	+0.941	-0.059
	$n_{N9} \rightarrow n_{Li}^*$	0.025	8.35		
7a	$n_{N7} \rightarrow n_{Li}^*$	0.021	7.77	+0.954	-0.046
	$n_{O6} \rightarrow n_{Li}^*$	0.019	7.65		
8a	$n_{N3} \rightarrow n_{Li}^*$	0.025	8.98	+0.952	-0.048
	$n_{N2} \rightarrow n_{Li}^*$	0.018	6.34		
10a	$n_{N3} \rightarrow n_{Li}^*$	0.019	6.60	+0.951	-0.049
	$n_{O2} \rightarrow n_{Li}^*$	0.016	7.21		
11a	$n_{N3} \rightarrow n_{Li}^*$	0.024	8.18	+0.952	-0.048
	$n_{N4} \rightarrow n_{Li}^*$	0.017	5.73		
12a	$n_{O4} \rightarrow n_{Li}^*$	0.009	5.84	+0.984	-0.016
13a	$n_{O2} \rightarrow n_{Li}^*$	0.011	7.01	+0.984	-0.016

stabilization energy (ΔE_{CT}) for three kinds of Li-complex species are also shown in Tables 6 to 8. Two quantities Δq_{CT} and Δq_{Li}^{NPA} in Li^+-DNA-*base* can correlate with each other with correlation coefficient, R^2, 0.937, as shown in Fig. 5, while the corresponding values for Li_3^+ and CH_3Li are 0.498 and 0.015, respectively. However, ΔE_{CT} is just one of components of interaction energy, other factors are also involved in the interaction mechanism. These effective factors can be such as the changes in polarization and deformation energy.

CONCLUSIONS

Interactions of three Li species Li^+, Li_3^+ and CH_3Li with the most stable tautomers of DNA-*base* have been investigated, systematically. The lithium affinities and thermodynamic functions show that the affinity of DNA-*bases* to Li^+ is higher than that in other species. Moreover, the lithium affinity order of DNA-*bases* is guanine > cytosine > adenine > thymine for Li^+ and Li_3^+ while in CH_3Li case is cytosine > guanine > adenine > thymine. In all cases, bidentate complexes have more lithium affinity

Table 7. Δq_{CT} (a.u.), ΔE_{CT} (kcal mol^{-1}) of Li_3^+, $q_{Li_3^+}$ (NPA Atomic Charge) and $\Delta q_{Li_3^+}$ of Li_3^+ Complexes in Accordance with Fig. 3

| Molecule	Donor to Acceptor	Δq_{CT}	ΔE_{CT}	$q_{Li_3^+}$	$\Delta q_{Li_3^+}$
1b	$n_{N7} \rightarrow n_{Li1}^*$	0.037	7.80	0.945	-0.055
	$n_{N6} \rightarrow n_{Li2}^*$	0.031	6.09		
2b	$n_{N1} \rightarrow n_{Li}^*$	0.051	9.04	0.955	-0.045
3b	$n_{N3} \rightarrow n_{Li}^*$	0.047	8.90	0.955	-0.045
4b	$n_{N7} \rightarrow n_{Li}^*$	0.044	8.49	0.961	-0.039
5b	$n_{N9} \rightarrow n_{Li1}^*$	0.037	7.78	0.938	-0.062
	$n_{N3} \rightarrow n_{Li2}^*$	0.037	7.61		
6b	$n_{N9} \rightarrow n_{Li1}^*$	0.033	7.52	0.932	-0.068
	$n_{N3} \rightarrow n_{Li2}^*$	0.047	8.99		
7b	$n_{N7} \rightarrow n_{Li1}^*$	0.020	6.27	0.943	-0.057
	$n_{O6} \rightarrow n_{Li2}^*$	0.025	10.37		
8b	$n_{N3} \rightarrow n_{Li1}^*$	0.040	7.86	0.948	-0.052
	$n_{N2} \rightarrow n_{Li2}^*$	0.036	8.33		
9b	$n_{N3} \rightarrow n_{Li}^*$	0.050	9.16	0.949	-0.051
10b	$n_{O2} \rightarrow n_{Li1}^*$	0.021	6.70	0.941	-0.059
11b	$n_{N3} \rightarrow n_{Li}^*$	0.019	6.25	0.968	-0.032
12b	$n_{O4} \rightarrow n_{Li}^*$	0.023	7.95	0.968	-0.032
13b	$n_{O2} \rightarrow n_{Li}^*$	0.024	8.45	0.970	-0.030

and the carbonyl oxygen is generally preferred over amino nitrogen. Those complexes with the Li-O interaction have more interaction energies in comparison with Li-N containing interactions. The trend for lithium affinity in three different Li species is generally as $Li^+ > Li_3^+ > CH_3Li$. The ΔS^{298} value for Li^+ complexation reaction is slightly similar for all DNA-*base* tautomers while the relative differences between tautomers are not negligible for two other reactions.

The computed results of QTAIM confirm that all Li-DNA-*base* interactions are electrostatic bond. More positive $\nabla^2 \rho_{BC}$ in Li^+ complexes reveals the stronger electrostatic interaction. Li^+ and Li_3^+ tend to have bidentate complexes with particular tautomers while CH_3Li prefers mono-coordinated ones. BCPs detected by QTAIM also show this tendency.

NBO analysis conforms the results of thermodynamics and QTAIM. NBO also show a reasonable charge transfer

Table 8. Δq_{CT} (a.u.), ΔE_{CT} (kcal mol^{-1}), NPA Atomic Charges q_{Li}, q, Δq_u and Δq_C of CH_3Li Complexes in Accordance with Fig. 4

Molecule	Donor to acceptor	Δq_{CT}	ΔE_{CT}	q_{Li}	Δq_u	q_C	Δq_C
1c	$n_{N7} \rightarrow n_{Li}^*$	0.039	14.48	+0.855	-0.002	-1.399	0.009
2c	$n_{N1} \rightarrow n_{Li}^*$	0.038	13.73	+0.871	0.014	-1.403	0.005
3c	$n_{N3} \rightarrow n_{Li}^*$	0.036	13.01	+0.883	0.026	-1.390	0.018
4c	$n_{N7} \rightarrow n_{Li}^*$	0.039	14.48	+0.855	-0.002	-1.399	0.009
5c	$n_{N3} \rightarrow n_{Li}^*$	0.038	13.23	+0.788	-0.069	-1.356	0.052
6c	$n_{N3} \rightarrow n_{Li}^*$	0.038	13.55	+0.883	0.026	-1.382	0.026
7c	$n_{O6} \rightarrow n_{Li}^*$	0.029	14.44	+0.835	-0.022	-1.376	0.032
8c	$n_{N3} \rightarrow n_{Li}^*$	0.055	17.67	+0.797	-0.060	-1.379	0.029
9c	$n_{N3} \rightarrow n_{Li}^*$	0.053	17.53	+0.773	-0.084	-1.356	0.052
10c	$n_{O2} \rightarrow n_{Li}^*$	0.031	15.11	+0.830	-0.027	-1.375	0.033
11c	$n_{N3} \rightarrow n_{Li}^*$	0.036	12.95	+0.884	0.027	-1.387	0.021
12c	$n_{O4} \rightarrow n_{Li}^*$	0.030	14.81	+0.831	-0.026	-1.377	0.031
13c	$n_{O2} \rightarrow n_{Li}^*$	0.028	15.41	+0.824	-0.033	-1.371	0.037
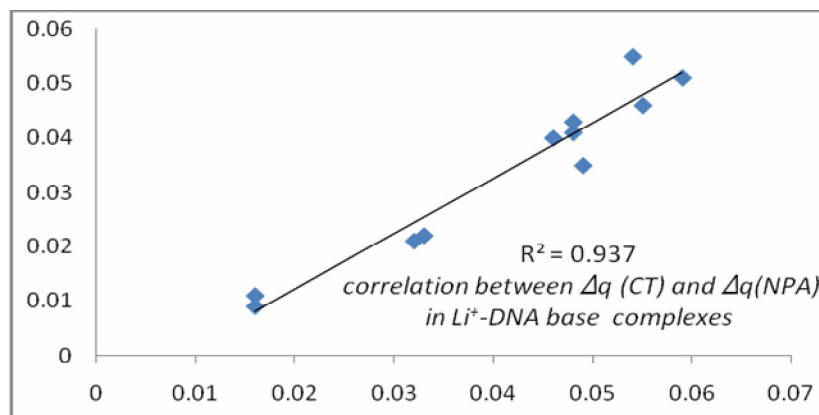
Fig. 5. Correlation diagram between $\Delta q(CT)$ and $\Delta q(NPA)$.

as expected.

REFERENCES

[1]   G.L. Eichhorn, Adv. Inorg. Biochem. 3 (1981) 1.

[2]   S.J. Lippard, J.M. Berg, Principle of Bioinorganic Chemistry, University Science Books, Mill Valley, CA, 1994.

[3]   W. Kaim, B. Schwedersky, Bioinorganic Chemistry, Inorganic Elements in the Chemistry of Life, John Wiley & Sons, Chichesta, 1994.

[4]   L.A. Loeb, A.R. Zakour, in: T.G. Spiro (Ed.), Nucleic Acid-Metal Ion Interactions, John Wiley & Sons, New York, 1980,

[5]   G.L. Eichhorn, in: G.L. Eichhorn (Ed.), In Inorganic Biochemistry, Elsevier, New York, 1973.

[6]   E.H.S. Anwander, M.M. Probst, B.M. Rode, Bipolymers 29 (1990) 757.

[7]   W.R. Rodwell, L. Radom, J. Am. Chem. Soc. 103 (1981) 2865.

[8]   J.V. Burda, J. Šponer, P. Hobza, J. Phys. Chem. 100 (1996) 7250.

[9]   M.P. Chiarelli, M.L. Gross, J. Phys. Chem. 93 (1989) 3595.

[10]   C. Colominas, F.J. Luque, M. Orozco, J. Am. Chem. Soc. 118 (1996) 6811.

[11]   B.A. Cerda, C. Wesdemiotis, J. Am. Chem. Soc. 117 (1995) 9734.

[12]   M.T. Rodgers, P.B. Armentrout, J. Am. Chem. Soc. 122 (2000) 8548.

[13]   G.Y. Lee, Bull. Korean Chem. Soc. 23 (2002) 1023.

[14]   N. Russo, M. Toscano, A. Grand, J. Phys. Chem. B 105 (2001) 4735.

[15]   M. Meyer, J.J. Suhnel, Biomol. Struct. Dyn. 20 (2003) 507.

[16]   B.A. Cerda, C. Wesdemiotis, J. Am. Chem. Soc. 118 (1996) 11884.

[17]   J.L. Aubagnac, T.M. Devienne, R. Combarieu, J.L. Barascut, J.L. Imbach, H.B. Lazrek, Org. Mass. Spectrom. 18 (1983) 361.

[18]   D.A. McCrery, M.L. Gross, Anal. Chim. Acta 178 (1985) 91.

[19]   K.B. Tomer, M.L. Gross, Anal. Chem. 58 (1986) 2527.

[20]   A.M. Hogg, J.G. Kelland, C.J. Vederas, V. Hel, Chim. Acta 69 (1986) 908.

[21]   R.D. Voyksner, Org. Mass. Spectrom. 22 (1987) 513.

[22]   K.P. Madhusudanan, S.B. Katti, S.A.N. Hashmi, Org. Mass. Spectrom. 28 (1993) 970.

[23]   G.J.C. Paul, T. Theophanides, J. Anastassopoulou, I. Marcotte, M. Bertrand, Proceedings of the 43th ASMS Conference on Mass Spectrometry and Allied Topics, May 21-26, Atlanta, GA, 1995, p. 608.

[24]   M.T. Rodgers, P.B. Armentrout, Proceedings of the 44th ASMS Conference on Mass Spectrometry and Allied Topics, Portland, OR, 1996, p. 88.

[25]   T. Mourik, J.D. Dingley, Chem. Eur. J. 11 (2005) 6064.

[26]   A.C. Plaush, R.R. Sharp, J. Am. Chem. Soc. 98 (1976) 7973.

[27]   J.E. Del Bene, J. Phys. Chem. 88 (1984) 5927.

[28]   W. Zhu, X. Luo, C.M. Puah, X. Tan, J. Shen, J. Gu, K. Chen, H. Jiang, J. Phys. Chem. A 108 (2004) 4008.

[29]   L. Sun, Y. Bu, J. Phys. Chem. B 109 (2005) 593.

[30]   Y. Zhao, L. Zhou, Fuzhou Daxue Xuebao 32 (2004) 201.

[31]   J. Reynisson, S. Steenken, J. Mol. Struct. (Theochem.) 635 (2003) 133.

[32]   S.M. Hashemianzadeh, S. Faraji, A.H. Amin, S. Ketabi, Monatshefte für Chemie 139 (2008) 89.

[33]   M.Y. Chou, M.L. Cohen, Phys. Lett. 113 (1986) 420.

[34]   K. Clemenger, Phys. Rev. B 32 (1985) 1359.

[35]   K. Selby, M. Vollmer, J. Masui, V. Kresin, W.A. de Heer, W.D. Knight, Phys. Rev. B 40 (1989) 5417.

[36]   D.S. Sapse, E. Champeil, J. Maddaluno, C. Fressigné, A.M. Sapse, C.R. Chim. 11 (2008) 1262.

[37]   R.F.W. Bader, Chem. Rev. 91 (1991) 893.

[38]   R.F.W. Bader, Atoms in Molecules, A Quantum Theory, Oxford University Press, Oxford, 1990.

[39]   A.E. Reed, L.A. Curtiss, F. Weinhold, Chem. Rev. 88 (1988) 899.

[40]   F. Weinhold, in: Pv.R. Schleyer, N.L. Allinger, P.A. Kollmann, T. Clark, H.F.S. Schaefer, J. Gasteiger, P.R. Schreiner (Eds.), Encyclopedia of Computational Chemistry, Wiley-VCH, Chichester, 3 (1998) 1792.

[41]   M.J. Frisch, *et al.* Gaussian 03, Revision B.04,

Gaussian, Inc., Pittsburgh PA, 2003.

[42] R.D.D. Dennington II, T.A. Keith, J.M. Millan, Gauss View 03, Gaussian, Inc., Pittsburgh PA, 2003.

[43] A.D. Becke, J. Chem. Phys. 98 (1993) 5648.

[44] C. Lee, W. Yang, R.G. Parr, Phys. Rev. B 37 (1988) 785.

[45] A.E. Reed, R.B. Weinstock, F. Weinhold, J. Chem. Phys. 83 (1985) 735.

[46] F. Biegler-König, Schönbohm, AIM2000 Program, Ver 2.0, 2002.

[47] P.B. Armentrout, J. Am. Soc. Mass Spec. 11 (2000) 371.

[48] R.F.W. Bader, J. Phys. Chem. A 102 (1998) 7314.

[49] D. Cremer, E. Kraka, Angew. Chem. Int. Ed. 23 (1984) 627.